



# $\gamma$ -Fe<sub>2</sub>O<sub>3</sub>@SiO<sub>2</sub>- $\gamma$ -aminobutyric acid as a novel superparamagnetic nanocatalyst promoted green synthesis of chromeno[4,3,2-*de*][1,6]-naphthyridine derivatives

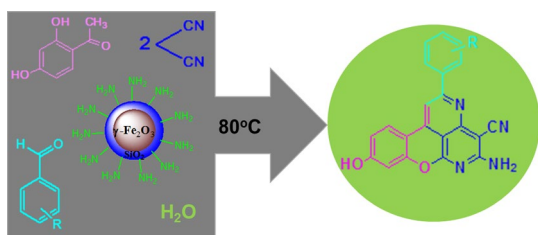
Hadi Mohammadi<sup>1</sup> · Hamid Reza Shaterian<sup>1</sup>

Received: 22 June 2018 / Accepted: 10 October 2018  
© Springer-Verlag GmbH Austria, part of Springer Nature 2018

## Abstract

Grafting of  $\gamma$ -aminobutyric acid on the superparamagnetic  $\gamma$ -Fe<sub>2</sub>O<sub>3</sub>@SiO<sub>2</sub> nanoparticles afforded  $\gamma$ -Fe<sub>2</sub>O<sub>3</sub>@SiO<sub>2</sub>- $\gamma$ -aminobutyric acid as a novel heterogeneous nanocatalyst, which was characterized by X-ray diffraction, Fourier transform-infrared spectroscopy, vibrating sample magnetometry, field emission scanning electron microscopy, energy-dispersive X-ray spectroscopy, and thermal analysis. In this research, we report a convenient and one-pot efficient direct protocol for the pseudo four-component preparation of chromeno[4,3,2-*de*][1,6]naphthyridine derivatives via cascade condensation reaction of malononitrile, 2,4-dihydroxyacetophenone with various aromatic aldehydes in the presence of the catalytic amount of the  $\gamma$ -Fe<sub>2</sub>O<sub>3</sub>@SiO<sub>2</sub>- $\gamma$ -aminobutyric acid under green conditions in aqueous media. This procedure offers several advantages such as: very easy reaction conditions, simple work-up, or purification, excellent yields, high purity of the desired product, atom economy, and short reaction times. The superparamagnetic nanocatalyst is magnetically separable and kept stability after recycling for at least five consecutive runs without detectable activity loss.

## Graphical abstract



**Keywords**  $\gamma$ -Fe<sub>2</sub>O<sub>3</sub>@SiO<sub>2</sub>- $\gamma$ -aminobutyric acid · Superparamagnetic nanocatalyst · Chromeno[4,3,2-*de*][1,6]-naphthyridines · Multi-component reactions · Water

**Electronic supplementary material** The online version of this article (<https://doi.org/10.1007/s00706-018-2317-5>) contains supplementary material, which is available to authorized users.

✉ Hamid Reza Shaterian  
hrshaterian@chem.usb.ac.ir

<sup>1</sup> Department of Chemistry, Faculty of Sciences, University of Sistan and Baluchestan, PO Box 98135-674, Zahedan, Iran

## Introduction

The fields of organometallic compounds with the wide variety of structures have been high-fast developing in the chemistry [1–4]. Nano-superparamagnetic organometallic compounds are considered as a very important class of materials, which have wide broad applications in many biological aspects [5–8]. Nano-superparamagnetic transition metal oxides such as iron are one of the most adjustable systems which have also applications in medical, industrial, and biological in addition to their important

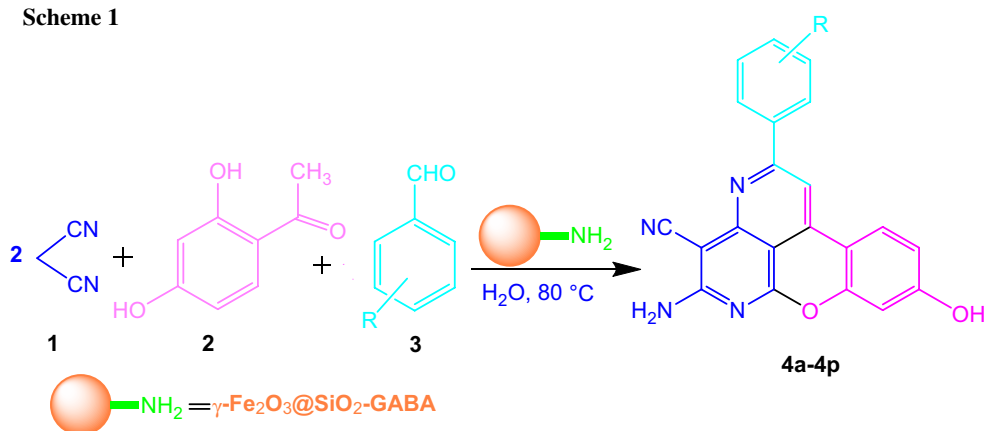
roles in catalysis and organic synthesis [9–12]. Studies of new kind of organometallic compounds grafting of organocatalysts on the superparamagnetic,  $\gamma\text{-Fe}_2\text{O}_3@$   $\text{SiO}_2$ , nanoparticles were attracting the consideration of researchers in organic chemistry [13–16]. In the present research, we report preparation of  $\gamma\text{-Fe}_2\text{O}_3@$   $\text{SiO}_2$ - $\gamma$ -aminobutyric acid ( $\gamma\text{-Fe}_2\text{O}_3@$   $\text{SiO}_2$ -GABA) for the first time. This superparamagnetic organometallic compound as catalyst was applied for synthesis a series of chromeno[4,3,2-*de*][1,6]naphthyridines compounds from cascade pseudo four-component condensation reaction of malononitrile, 2,4-dihydroxyacetophenone with various aromatic aldehydes (Scheme 1).

## Results and discussion

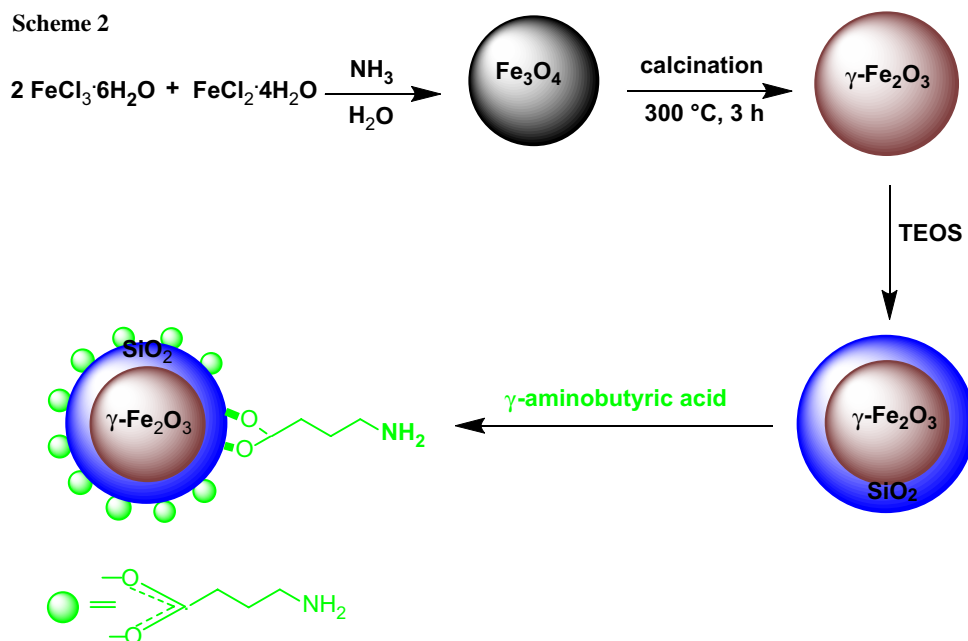
$\gamma\text{-Fe}_2\text{O}_3@$   $\text{SiO}_2$ -GABA as a new nanocatalyst was synthesized based on the following procedure (Scheme 2). First, superparamagnetic  $\text{Fe}_3\text{O}_4$  nanoparticles were facilely prepared by a chemical co-precipitating method [17]. Second,  $\text{Fe}_3\text{O}_4$  nanoparticles were converted into  $\gamma\text{-Fe}_2\text{O}_3$  at 300 °C for 3 h. Then,  $\gamma\text{-Fe}_2\text{O}_3$  was encapsulated by  $\text{SiO}_2$  as  $\gamma\text{-Fe}_2\text{O}_3@$   $\text{SiO}_2$  using tetraethyl orthosilicate (TEOS) [18]. Finally, the reaction of GABA with  $\gamma\text{-Fe}_2\text{O}_3@$   $\text{SiO}_2$  formed a superparamagnetic  $\gamma\text{-Fe}_2\text{O}_3@$   $\text{SiO}_2$ -GABA as the new nanocatalyst.

The magnetic nanocatalyst was characterized using different techniques such as X-ray diffraction (XRD), Fourier transform-infrared spectroscopy (FT-IR), field emission scanning electron microscopy (FE-SEM), energy-dispersive

Scheme 1



Scheme 2



X-ray spectroscopy (EDS), vibrating sample magnetometry (VSM), and thermal analysis (TGA). The XRD patterns of  $\gamma$ -Fe<sub>2</sub>O<sub>3</sub>,  $\gamma$ -Fe<sub>2</sub>O<sub>3</sub>@SiO<sub>2</sub>, and  $\gamma$ -Fe<sub>2</sub>O<sub>3</sub>@SiO<sub>2</sub>-GABA had six characteristic peaks which have a good accordance with the cubic structure of maghemite ( $\gamma$ -Fe<sub>2</sub>O<sub>3</sub>) (JCPDS file No 04-0755). The positions of all the peaks indicated retention of the crystalline structure during functionalization of the  $\gamma$ -Fe<sub>2</sub>O<sub>3</sub> and the grafting process did not change phase of the  $\gamma$ -Fe<sub>2</sub>O<sub>3</sub> nanoparticles. The XRD pattern of  $\gamma$ -Fe<sub>2</sub>O<sub>3</sub>@SiO<sub>2</sub> and  $\gamma$ -Fe<sub>2</sub>O<sub>3</sub>@SiO<sub>2</sub>-GABA showed that SiO<sub>2</sub> and GABA formed amorphous phase which their patterns showed only pattern of crystalline  $\gamma$ -Fe<sub>2</sub>O<sub>3</sub> nanoparticles (Fig. 1).

We provided FE-SEM image from  $\gamma$ -Fe<sub>2</sub>O<sub>3</sub>@SiO<sub>2</sub>-GABA. Figure 2a represents the SEM image of  $\gamma$ -Fe<sub>2</sub>O<sub>3</sub>@SiO<sub>2</sub>-GABA which shows spherical morphology and average size 13 nm of nanoparticles using histogram curve Fig. 2b. Superparamagnetic  $\gamma$ -Fe<sub>2</sub>O<sub>3</sub> is encapsulated into SiO<sub>2</sub>. It separates organocatalyst by an external magnet and provides easy work-up; also, SiO<sub>2</sub> shell prevents agglomeration (large chunks) of spheres of nanoparticles before and after the reaction.

The components of the  $\gamma$ -Fe<sub>2</sub>O<sub>3</sub>@SiO<sub>2</sub>-GABA were also analyzed using energy-dispersive X-ray spectroscopy (EDS). EDS basically gives elemental information for qualitative analysis [19]. The EDS spectrum in Fig. 3 implicates the presence of atoms Fe, O, Si, C, and N in the catalyst which confirms the structure of organometallic compound.

The VSM diagram shows the magnetic properties of synthesis catalyst (Fig. 4). The hysteresis loop of the  $\gamma$ -Fe<sub>2</sub>O<sub>3</sub>@SiO<sub>2</sub>-GABA was measured. Magnetization (emu g<sup>-1</sup>) as a function of applied field (Oe) was depicted in Fig. 4 with the confined field from -10,000 to +10,000 Oe. Superparamagnetic behavior of the  $\gamma$ -Fe<sub>2</sub>O<sub>3</sub>@SiO<sub>2</sub>-GABA illustrates small

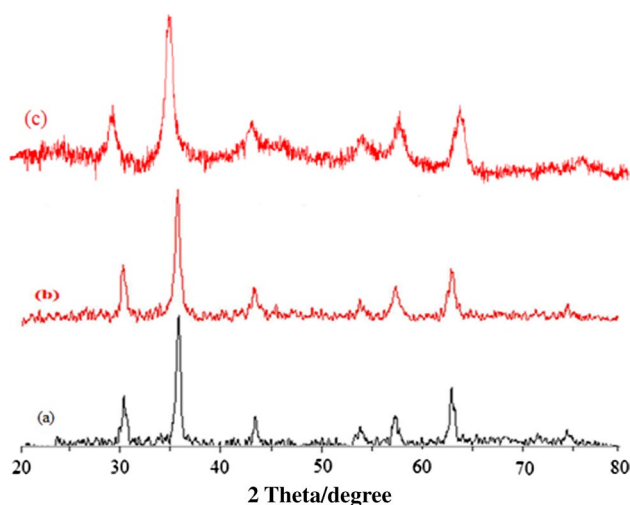


**Fig. 1** XRD pattern of **a**  $\gamma$ -Fe<sub>2</sub>O<sub>3</sub>; **b**  $\gamma$ -Fe<sub>2</sub>O<sub>3</sub>@SiO<sub>2</sub>; **c**  $\gamma$ -Fe<sub>2</sub>O<sub>3</sub>@SiO<sub>2</sub>-GABA

nanoparticles size of the catalyst. As it can be observed, saturation magnetization value of  $\gamma$ -Fe<sub>2</sub>O<sub>3</sub>@SiO<sub>2</sub>-GABA is 57 amu g<sup>-1</sup>.

The thermal stability of the  $\gamma$ -Fe<sub>2</sub>O<sub>3</sub>@SiO<sub>2</sub>-GABA was investigated by TGA analysis (Fig. 5). Small weight loss occurs below 200 °C, which is due to physically adsorbed solvent and water. There are two exothermic peaks accompanied with a mass loss of 7.5% in the temperature range of 200–550 °C in the TGA curve of  $\gamma$ -Fe<sub>2</sub>O<sub>3</sub>@SiO<sub>2</sub>-GABA. These peaks were mainly attributed to the decomposition of organic groups (GABA) grafted to the  $\gamma$ -Fe<sub>2</sub>O<sub>3</sub>@SiO<sub>2</sub> surface. The peak higher than 550 °C most probably corresponds to a phase transition in which the amorphous phase is converted into a crystalline phase. The total weight loss was computed to be 7.5% and the amount of GABA loaded on  $\gamma$ -Fe<sub>2</sub>O<sub>3</sub>@SiO<sub>2</sub> was equal to 0.72 mmol g<sup>-1</sup>.

The characterization of  $\gamma$ -Fe<sub>2</sub>O<sub>3</sub>@SiO<sub>2</sub>-GABA as nanocatalyst was also confirmed by FT-IR spectrum. The peak at 3400 cm<sup>-1</sup> was probably attributed to the NH<sub>2</sub> groups, which is overlapped by the O–H stretching vibration. C–H stretching vibrations appear at 2930 cm<sup>-1</sup>. The Fe–O stretching vibration was observed at 550–650 cm<sup>-1</sup> and stretching mode of Si–O–Si showed a strong broad peak at about 1099–1220 cm<sup>-1</sup> (Fig. 6).

To evaluate the activity of the catalyst, the pseudo four-component reaction of 2,4-dihydroxyacetophenone, malononitrile, and benzaldehyde was selected as a model to optimize the reaction conditions (Scheme 3).

The reaction was carried out in the presence of  $\gamma$ -Fe<sub>2</sub>O<sub>3</sub>@SiO<sub>2</sub>-GABA, Fe<sub>3</sub>O<sub>4</sub> NMPs,  $\gamma$ -Fe<sub>2</sub>O<sub>3</sub>,  $\gamma$ -Fe<sub>2</sub>O<sub>3</sub>@SiO<sub>2</sub>, citric acid, sulfamic acid, InCl<sub>3</sub>, GABA, silica gel, and FeCl<sub>3</sub>·6H<sub>2</sub>O at 80 °C in aqueous media. The results are summarized in Table 1. With regard to the results in Table 1, it was observed that nano-catalysts have shown better conditions than other types of catalysts in the preparation of chromeno[4,3,2-*de*]-[1,6]naphthyridine derivatives. Table 1 also shows that sequence activities of various nano-catalysts are  $\gamma$ -Fe<sub>2</sub>O<sub>3</sub>@SiO<sub>2</sub>-GABA >  $\gamma$ -Fe<sub>2</sub>O<sub>3</sub>@SiO<sub>2</sub> >  $\gamma$ -Fe<sub>2</sub>O<sub>3</sub> > Fe<sub>3</sub>O<sub>4</sub>. GABA as catalyst showed the catalytic activity for this reaction but moderate yields and no reusability of GABA are disadvantages of it.  $\gamma$ -Fe<sub>2</sub>O<sub>3</sub>@SiO<sub>2</sub>-GABA nanocatalyst has several advantages in the synthesis of chromeno[4,3,2-*de*]-[1,6]naphthyridine derivatives, such as good yields, short reaction times, less amount of the catalyst, and excellent reusability (Table 1).

To select the appropriate solvent, various solvents such as CH<sub>2</sub>Cl<sub>2</sub>, CH<sub>3</sub>CN, ethanol, water, mixtures of water:ethanol, and also under solvent-free conditions, were used in the model reaction in the presence of  $\gamma$ -Fe<sub>2</sub>O<sub>3</sub>@SiO<sub>2</sub>-GABA (7 mg). The results are shown in Table 2. According to the results, the highest yield of product and maximum performance of the catalyst were obtained, once the reaction was carried out in water as a solvent. The reaction completed

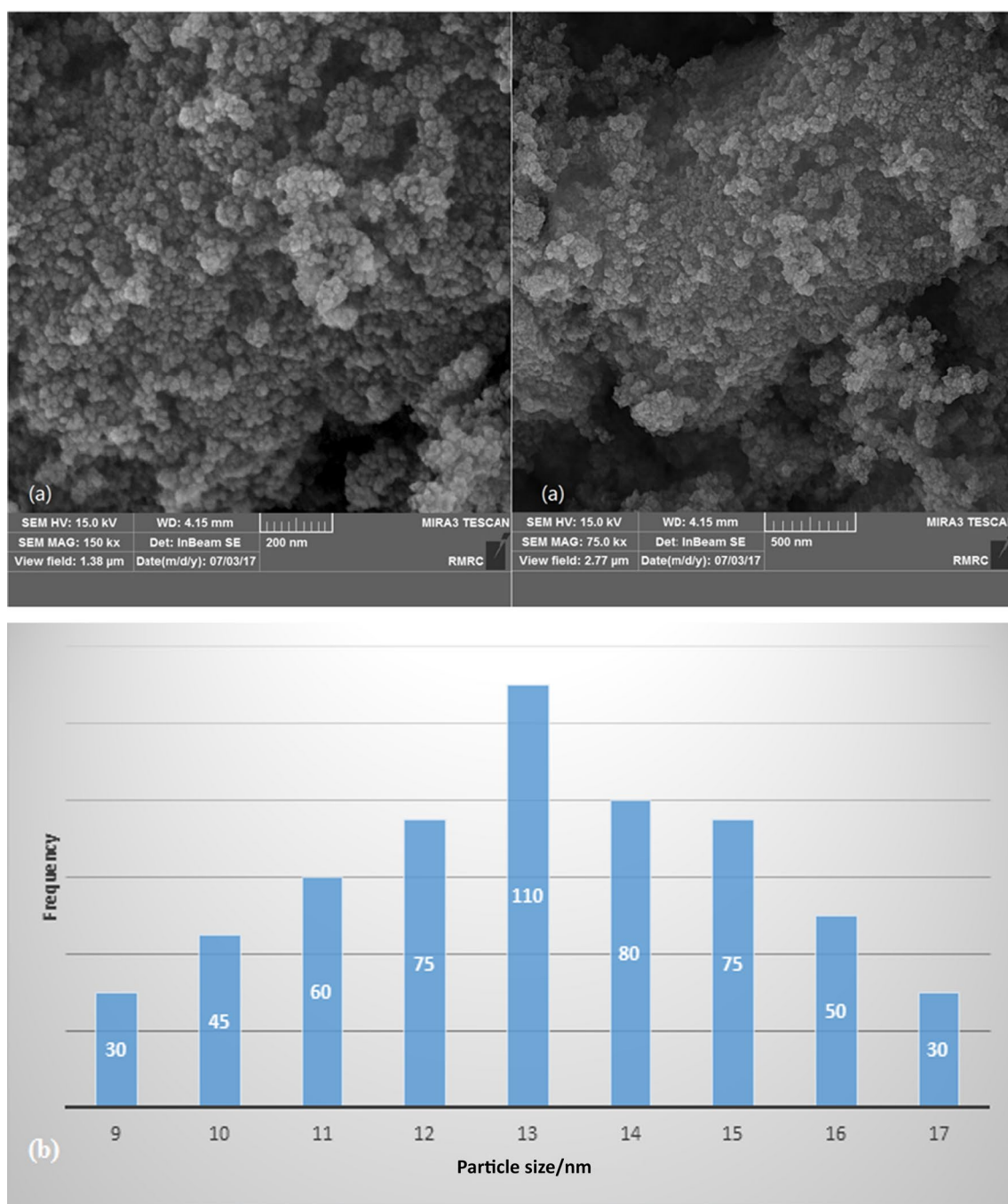


**Fig. 2** **a** FE-SEM image of MNPs-GABA; **b** particle size distribution histogram of  $\gamma\text{-Fe}_2\text{O}_3\text{@SiO}_2\text{-GABA}$

in 50 min and excellent yield (92%) of the product was obtained in water (Table 2, entry 5). The important role of performance of the catalyst in water was the formation of hydrogen bonds between starting materials and water. A significant decrease in yields was observed when  $\text{CH}_2\text{Cl}_2$ ,  $\text{CH}_3\text{CN}$ , ethanol were used as the organic reaction solvent. Moreover, reaction performed was drastically decreased with further increase in ethanol in water (Table 2, entries 6, 7).

To optimize the amount of the  $\gamma\text{-Fe}_2\text{O}_3\text{@SiO}_2\text{-GABA}$  as catalyst in the reaction model, the reaction was carried out in presence of the various amounts of the catalyst at 80 °C in water as solvent (Table 3, entries 1–5). The use of 7 mg of the catalyst in the reaction is sufficient for achieving the best yield of the desired product. For selecting the best temperature, the reaction was performed at different temperatures (Table 3, entries 3, 6–8) in the presence of  $\gamma\text{-Fe}_2\text{O}_3\text{@}$

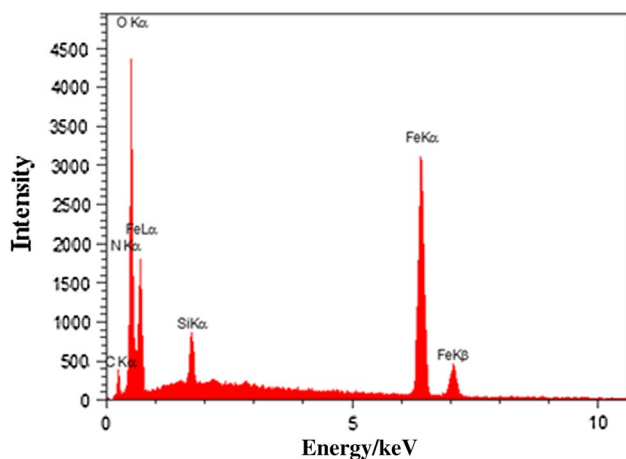


Fig. 3 EDS spectrum of  $\gamma$ -Fe<sub>2</sub>O<sub>3</sub>@SiO<sub>2</sub>-GABA

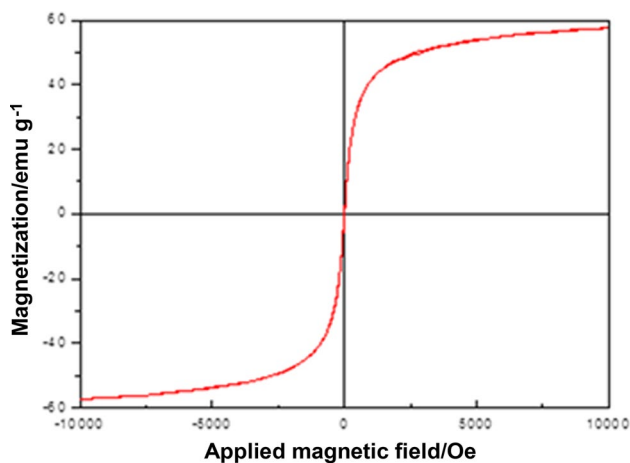


Fig. 4 VSM diagrams of  $\gamma$ -Fe<sub>2</sub>O<sub>3</sub>@SiO<sub>2</sub>-GABA

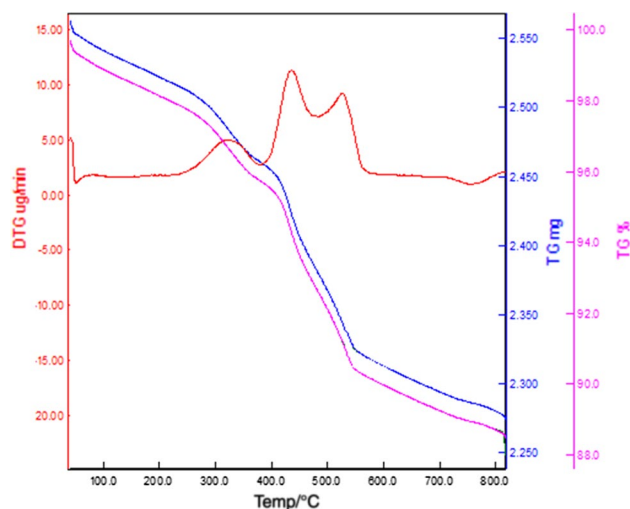


Fig. 5 Thermogravimetric analysis of  $\gamma$ -Fe<sub>2</sub>O<sub>3</sub>@SiO<sub>2</sub>-GABA

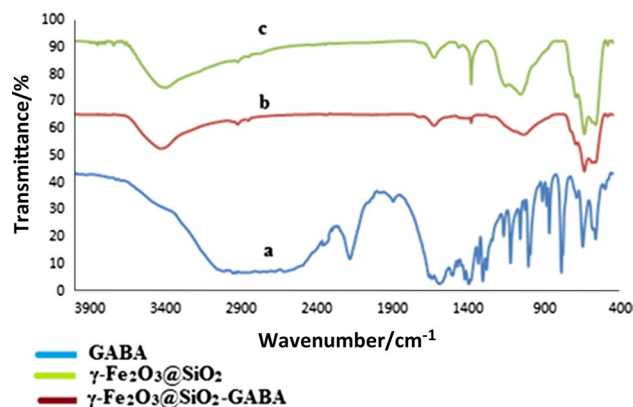


Fig. 6 FT-IR spectra: (a) GABA; (b)  $\gamma$ -Fe<sub>2</sub>O<sub>3</sub>@SiO<sub>2</sub>; (c)  $\gamma$ -Fe<sub>2</sub>O<sub>3</sub>@SiO<sub>2</sub>-GABA

SiO<sub>2</sub>-GABA (7 mg) in water. The best result was obtained at 80 °C (Table 3, entry 3).

According to optimal considered conditions (7 mg  $\gamma$ -Fe<sub>2</sub>O<sub>3</sub>@SiO<sub>2</sub>-GABA, reaction temperature 80 °C in water as green solvent), some new chromeno[4,3,2-*de*][1,6]naphthyridine derivatives were synthesized and results are shown in Table 4. The obtained results indicate that the reactions can proceed well enough with a relatively wide range of aromatic-substituted benzaldehydes containing electron-donating and electron-withdrawing groups.

According to the literature [21], the proposed mechanism for the formation of the product is shown in Scheme 4. First, chalcone **I** was formed through the aldol condensation between benzaldehydes **3** and 2,4-dihydroxyacetophenone (**2**). Next, Knoevenagel product **II** was obtained from the reaction of malononitrile with chalcone **I**. In the following, the intramolecular nucleophilic attack by the enolic OH group of **II** leads to formation of the intermediate **III**. The condensation reaction of **III** with second molecule of malononitrile produces the intermediate **IV**. Subsequently, the intramolecular cyclization of **IV** followed by aromatization formed the final product.

GABA as organocatalyst can be separated easily by an external magnet when it supports on superparamagnetic of  $\gamma$ -Fe<sub>2</sub>O<sub>3</sub> nanoparticles. GABA bonded to  $\gamma$ -Fe<sub>2</sub>O<sub>3</sub>@SiO<sub>2</sub> from carboxylic acid side and amino group acts as basic catalyst.  $\gamma$ -Fe<sub>2</sub>O<sub>3</sub>@SiO<sub>2</sub>-GABA provides a simple work-up that causes high yields of isolated pure products. Superparamagnetic  $\gamma$ -Fe<sub>2</sub>O<sub>3</sub> is encapsulated into SiO<sub>2</sub>.  $\gamma$ -Fe<sub>2</sub>O<sub>3</sub>@SiO<sub>2</sub>-GABA as a heterogenous basic nanocatalyst acts well in the reactions and produces desired products in high yields after purification by a simple work-up.

As shown in Fig. 7,  $\gamma$ -Fe<sub>2</sub>O<sub>3</sub>@SiO<sub>2</sub>-GABA can act as an effective catalyst with respect to the reaction time, yield of the product, TON (turnover number) and TOF (turnover frequency) and the recyclability of  $\gamma$ -Fe<sub>2</sub>O<sub>3</sub>@SiO<sub>2</sub>-GABA was

Scheme 3

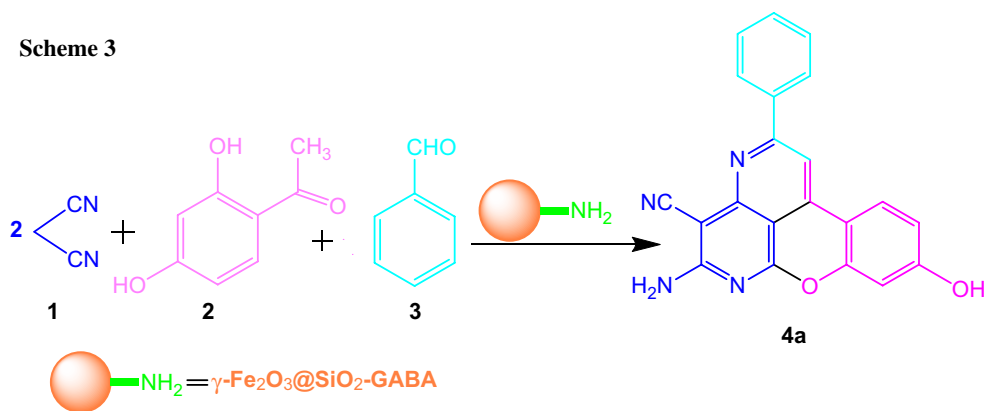


**Table 1** Preparation of 5-amino-9-hydroxy-2-phenylchromeno[4,3,2-*de*][1,6]naphthyridine-4-carbonitrile in the presence of  $\gamma\text{-Fe}_2\text{O}_3@ \text{SiO}_2\text{-GABA}$ ,  $\text{Fe}_3\text{O}_4$  NMPs,  $\gamma\text{-Fe}_2\text{O}_3$ ,  $\gamma\text{-Fe}_2\text{O}_3@ \text{SiO}_2$ , citric acid, sulfamic acid,  $\text{InCl}_3$ , GABA, silica gel, and  $\text{FeCl}_3 \cdot 6\text{H}_2\text{O}$  at 80 °C in aqueous media

Entry	Catalyst (amount) [Ref.]	Time/h	Yield/% <sup>a</sup>
1	$\text{FeCl}_3 \cdot 6\text{H}_2\text{O}$ (18 mg)	4	35
2	$\text{Fe}_3\text{O}_4$ NMPs (12 mg) [22]	4	60
3	GABA (35 mg)	4	45
4	$\gamma\text{-Fe}_2\text{O}_3$ NMPs (11 mg)	4	65
5	$\gamma\text{-Fe}_2\text{O}_3@ \text{SiO}_2$ NMPs (10 mg)	2	75
6	$\gamma\text{-Fe}_2\text{O}_3@ \text{SiO}_2\text{-GABA}$ (7 mg)	0.83	92
7	Silica gel (30 mg) [21]	2	67
8	$\text{InCl}_3$ (22 mg)	4	50
9	Sulfamic acid (25 mg)	4	55
10	Citric acid (60 mg)	4	50
11	–	9	35

Reaction conditions: benzaldehyde (1 mmol), malononitrile (2 mmol), and 2,4-dihydroxyacetophenone (1 mmol) in the presence of different catalysts at 80 °C in water as solvent

<sup>a</sup>Yields refer to isolated pure product

**Table 2** Preparation of 5-amino-9-hydroxy-2-phenylchromeno[4,3,2-*de*][1,6]naphthyridine-4-carbonitrile in the presence of  $\gamma\text{-Fe}_2\text{O}_3@ \text{SiO}_2\text{-GABA}$  (7 mg) in different solvents

Entry	Solvent	Time/min	Temperature/°C	Yield/% <sup>a</sup>
1	EtOH	80	80	60
2	$\text{CH}_3\text{CN}$	110	80	45
3	$\text{CH}_2\text{Cl}_2$	120	40	15
4	Neat (solvent-free)	50	90	70
5	$\text{H}_2\text{O}$	50	80	92
6	$\text{H}_2\text{O} : \text{EtOH}$ (50:50)	50	80	75
7	$\text{H}_2\text{O} : \text{EtOH}$ (30:70)	50	80	70
8	$\text{H}_2\text{O} : \text{EtOH}$ (70:30)	50	80	80

Reaction conditions: benzaldehyde (1 mmol), malononitrile (2 mmol), and 2,4-dihydroxyacetophenone (1 mmol) in the presence of  $\gamma\text{-Fe}_2\text{O}_3@ \text{SiO}_2\text{-GABA}$  (7 mg) as catalyst

<sup>a</sup>Yields refer to isolated pure product

**Table 3** Optimization conditions of the amount of the catalyst and also selecting the best temperature for the preparation of 5-amino-9-hydroxy-2-phenylchromeno[4,3,2-*de*][1,6]naphthyridine-4-carbonitrile in aqueous media

Entry	Catalyst/mg	Temperature/°C	Time/min	Yield/% <sup>a</sup>
1	3	80	70	75
2	5	80	70	82
3	7	80	50	92
4	9	80	50	92
5	11	80	50	89
6	7	60	70	73
7	7	70	60	83
8	7	90	50	92

Reaction conditions: benzaldehyde (1 mmol), malononitrile (2 mmol), and 2,4-dihydroxyacetophenone (1 mmol)

<sup>a</sup>Yields refer to isolated pure product

examined in the one-pot pseudo four-component synthesis of 5-amino-9-hydroxy-2-phenylchromeno[4,3,2-*de*][1,6]naphthyridine-4-carbonitrile under optimized conditions (Fig. 7). After completion of reaction, the reaction mixture was cooled to room temperature and the solid separated was filtered, ethanol was added to the reaction mixture and the  $\gamma\text{-Fe}_2\text{O}_3@ \text{SiO}_2\text{-GABA}$  was separated by external magnet. The catalyst was washed with ethanol for three times and dried. As it was shown in Fig. 7, at least even after five runs, catalytic activity and product yield have no significant loss. Thus, this catalyst can endure reaction conditions and remain stable.

## Conclusion

$\gamma\text{-Fe}_2\text{O}_3@ \text{SiO}_2\text{-GABA}$  as a novel organometallic heterogeneous nano-magnetic catalyst has been successfully synthesized and characterized by the several techniques such as XRD, FT-IR, VSM, FE-SEM, EDS, and TGA-DTG. This efficient nano-organometallic catalyst was

**Table 4** Synthesis of chromeno[4,3,2-*de*][1,6]-naphthyridine derivatives catalyzed by  $\gamma$ -Fe<sub>2</sub>O<sub>3</sub>@SiO<sub>2</sub>-GABA nanoparticles (7 mg) at 80 °C in water as green solvent (Scheme 1)

Entry	R	Product	Time/min	Yield/% <sup>a</sup>	TON <sup>b</sup> TOF <sup>c</sup> /h <sup>-1</sup>	Observed m.p./°C	Lit. m.p./°C
1	H	<b>4a</b>	50	92	184 221	> 300	> 300 [20]
2	4-Me	<b>4b</b>	45	93	186 248	> 300	> 300 [20]
3	4-MeO	<b>4c</b>	45	93	186 248	> 300	> 300 [21]
4	2-Me	<b>4d</b>	50	92	184 221	> 300	–
5	3-Me	<b>4e</b>	50	92	184 221	> 300	–
6	2-Cl	<b>4f</b>	55	90	180 197	> 300	–
7	2-Br	<b>4g</b>	55	90	180 197	> 300	–
8	4-Br	<b>4h</b>	55	90	180 197	> 300	–
9	4-Cl	<b>4i</b>	50	90	180 216	> 300	–
10	3-Br	<b>4j</b>	50	91	182 219	> 300	–
11	2-MeO	<b>4k</b>	50	90	180 216	> 300	–
12	2,3-(MeO) <sub>2</sub>	<b>4l</b>	55	89	178 195	> 300	–
13	3,4,5-(MeO) <sub>3</sub>	<b>4m</b>	60	89	178 178	> 300	–
14	3,4-(MeO) <sub>2</sub>	<b>4n</b>	60	87	174 174	> 300	–
15	2,5-(MeO) <sub>2</sub>	<b>4o</b>	60	86	172 172	> 300	–
16	3,4-(HO) <sub>2</sub>	<b>4p</b>	60	89	178 178	> 300	–

Reaction conditions: substituted benzaldehydes (1 mmol), malononitrile (2 mmol), 2,4-dihydroxyacetophenone (1 mmol) in 3 cm<sup>3</sup> water and 7 mg of the catalyst ( $\gamma$ -Fe<sub>2</sub>O<sub>3</sub>@SiO<sub>2</sub>-GABA)

<sup>a</sup>Yields refer to the isolated pure products

<sup>b</sup>TON (Turnover number)=mmol of desired product/mmol of GABA in the used catalyst. The mmol of –NH<sub>2</sub> group was equal to the mmol GABA which were loaded on  $\gamma$ -Fe<sub>2</sub>O<sub>3</sub>@SiO<sub>2</sub>. It was equal to 0.72 mmol g<sup>-1</sup> (calculated by TGA analysis)

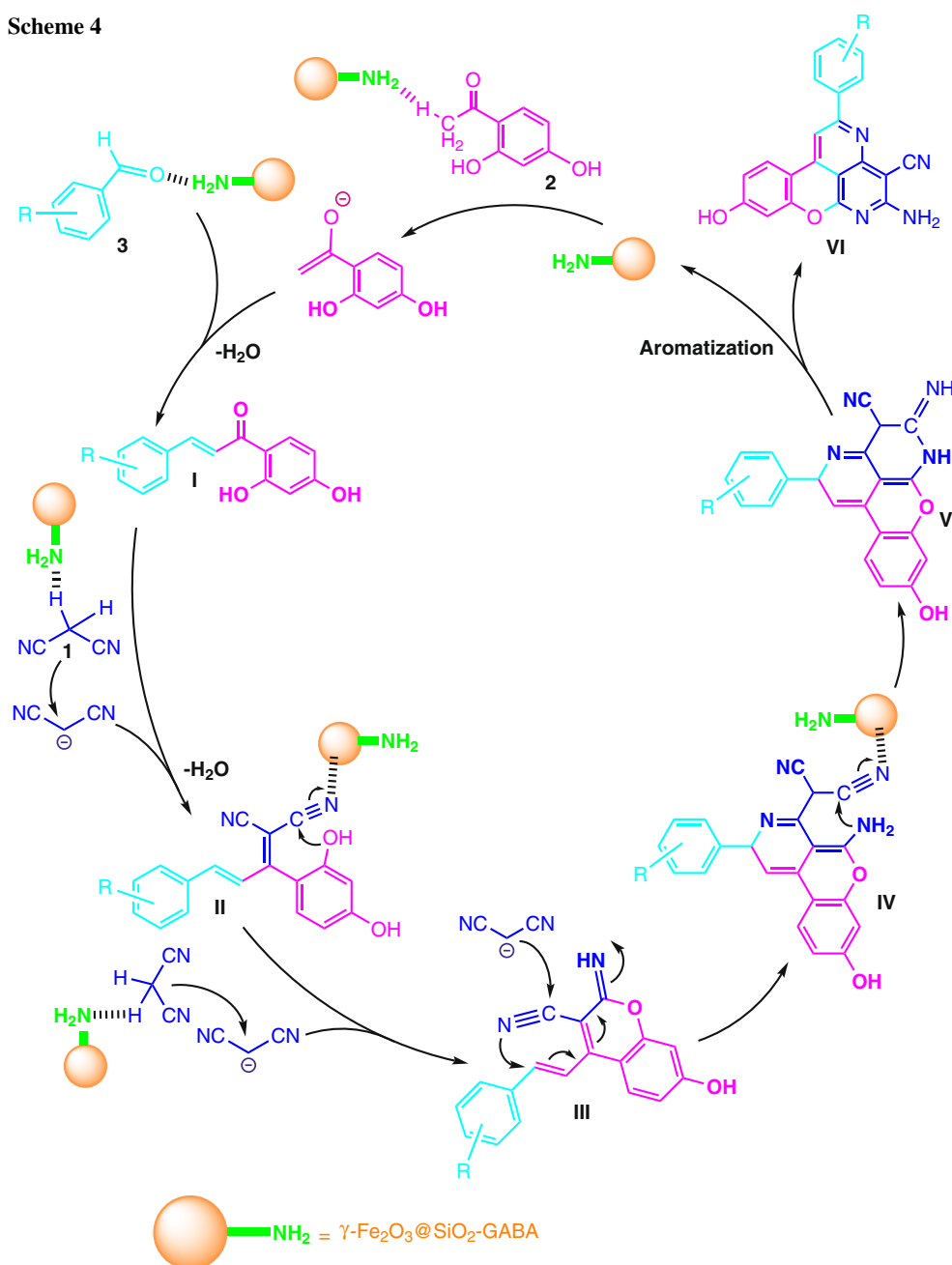
<sup>c</sup>TOF (Turnover frequency)=TON/reaction time (h)

successfully used for the pseudo four-component preparation of chromeno[4,3,2-*de*][1,6]naphthyridine derivatives under green conditions in aqueous media. Easy reaction conditions, simple work-up, or purification, excellent yields, high purity of the desired product, atom economy, and short reaction times are some advantages of this protocol. The superparamagnetic nanocatalyst is magnetically separable and stable in the reaction conditions without detectable activity loss.

## Experimental

All materials were purchased from Merck and Aldrich company. The NMR spectra were provided on Bruker Avance 300 MHz instruments in DMSO-*d*<sub>6</sub> as deuterated solvents. Melting points were determined in open capillaries using a BUCHI510 melting point apparatus. Thin-layer chromatography (TLC) was performed on silica-gel Poly

Scheme 4



Gram SIL G/UV 254 plates and progress of reactions was monitored by TLC. FT-IR spectra were recorded using KBr disks on a JASCO FT-IR 460 plus spectrophotometer. Elemental compositions were determined with a Leo 1450 VP scanning electron microscope equipped with an SC7620 energy-dispersive spectrometer (SEM-EDS) presenting a 133-eV resolution at 20 kV. Power X-ray diffraction (XRD) was performed on a Bruker D8-advance X-ray diffractometer with Cu K $\alpha$  ( $\lambda = 0.154$  nm) radiation. The magnetic property was measured by VSM/AGFM. TGA was done on a thermal analyzer with a heating rate of

10 °C min<sup>-1</sup> over a temperature range of 25–800 °C under flowing compressed N<sub>2</sub>.

### Preparation of GABA grafting $\gamma\text{-Fe}_2\text{O}_3@SiO_2$ magnetic nanoparticles

#### Preparation of $\gamma\text{-Fe}_2\text{O}_3$

The Fe<sub>3</sub>O<sub>4</sub> nanoparticles were prepared by literature procedure [17, 18]. FeCl<sub>2</sub>·4H<sub>2</sub>O (1.25 g, 6.28 mmol) and 3.33 g

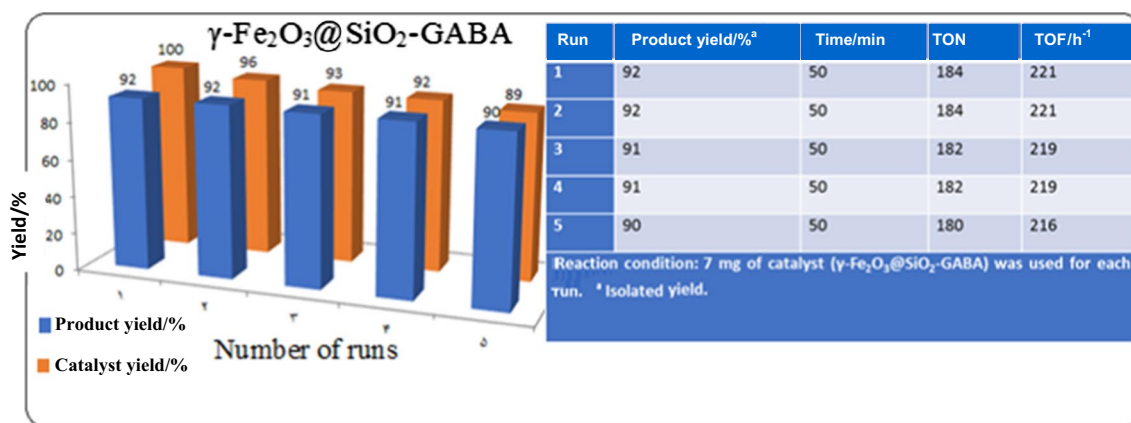


Fig. 7 Reusability of  $\gamma$ -Fe<sub>2</sub>O<sub>3</sub>@SiO<sub>2</sub>-GABA

FeCl<sub>3</sub>·6H<sub>2</sub>O (12.30 mmol) were dissolved in 80 cm<sup>3</sup> water separately, followed by the two iron salt solutions being mixed under continuous stirring (800 rpm). Then, 70 cm<sup>3</sup> aqueous ammonia solution (25%) was added dropwise to the stirring mixture at room temperature for 3 h and stirring continued for another hour. The black formed products as Fe<sub>3</sub>O<sub>4</sub> NMPs were collected by an external magnet. They were washed three times with water and ethanol and dried at 60 °C for 12 h. Fe<sub>3</sub>O<sub>4</sub> nanoparticles were heated at 300 °C in a furnace for 3 h. They were then converted into  $\gamma$ -Fe<sub>2</sub>O<sub>3</sub> nanoparticles.

### Preparation of $\gamma$ -Fe<sub>2</sub>O<sub>3</sub>@SiO<sub>2</sub>

$\gamma$ -Fe<sub>2</sub>O<sub>3</sub> nanoparticles (1 g) were dispersed in 40 cm<sup>3</sup> ethanol and the resulting mixture was stirred for 1 h at 40 °C. Subsequently, 2 cm<sup>3</sup> tetraethyl orthosilicate (TEOS) was charged to the reaction vessel and the mixture was continuously stirred for 24 h [18]. The silica-coated nanoparticles were collected by an external magnet, followed by washing three times with ethanol and drying at 70 °C in vacuum for 12 h.

### Preparation of $\gamma$ -Fe<sub>2</sub>O<sub>3</sub>@SiO<sub>2</sub>-GABA nanoparticles

$\gamma$ -Fe<sub>2</sub>O<sub>3</sub>@SiO<sub>2</sub> (800 mg) was dispersed in 80 cm<sup>3</sup> water under ultrasonic for 30 min. Subsequently, 1 g GABA was charged to the reaction vessel and the mixture was continuously stirred for 16 h at 90 °C.  $\gamma$ -Fe<sub>2</sub>O<sub>3</sub>@SiO<sub>2</sub>-GABA nanoparticles were removed from solution reaction by an external magnet and washed several times with water and ethanol and dried at 60 °C. The successful synthesis of this superparamagnetic nano-heterogeneous catalyst was characterized by several techniques such as XRD, FT-IR, VSM, FE-SEM, EDS, and TGA analysis. All results confirmed the structure of the  $\gamma$ -Fe<sub>2</sub>O<sub>3</sub>@SiO<sub>2</sub>-GABA.

### General procedure for the direct synthesis chromeno[1,6]naphthyridine derivatives using $\gamma$ -Fe<sub>2</sub>O<sub>3</sub>@SiO<sub>2</sub>-GABA nanoparticles as catalyst

Fe<sub>2</sub>O<sub>3</sub>@SiO<sub>2</sub>-GABA NMPs (7 mg) was added to a mixture of 2,4-dihydroxyacetophenone (1 mmol), malononitrile (2 mmol), and aromatic aldehydes (1 mmol) in 3 cm<sup>3</sup> water. The reaction mixture was stirred at 80 °C in an oil bath. The reaction was monitored by TLC. After completion of reaction, the reaction mixture was cooled to room temperature and the solid separated was filtered, and dissolved in ethanol to remove the catalyst by an external magnet and purified by crystallization in EtOH: DMF (10:1). The pure known products **4a–4c** were characterized and their physical data were compared with those of known compounds.

**5-Amino-9-hydroxy-2-(2-methylphenyl)chromeno[4,3,2-de]-[1,6]naphthyridine-4-carbonitrile (4d, C<sub>22</sub>H<sub>14</sub>N<sub>4</sub>O<sub>2</sub>)** Yellow solid; m.p.: > 300 °C; IR (KBr):  $\bar{\nu}$  = 3480, 3338, 3225, 2211 cm<sup>-1</sup>; <sup>1</sup>H NMR (300 MHz, DMSO-*d*<sub>6</sub>):  $\delta$  = 10.66 (1H, s), 8.18–8.20 (1H, d, *J* = 8.4 Hz), 7.67 (1H, s), 7.54–7.57 (1H, m), 7.44 (2H, s), 7.31–7.39 (3H, m), 6.81–6.84 (2H, m), 2.45 (3H, s) ppm; <sup>13</sup>C NMR (75 MHz, DMSO-*d*<sub>6</sub>):  $\delta$  = 166.43, 162.41, 162.11, 159.90, 155.68, 153.76, 140.39, 138.94, 136.45, 131.26, 130.07, 129.35, 126.95, 126.33, 117.13, 114.35, 109.13, 107.75, 103.86, 101.70, 76.00, 20.91 ppm.

**5-Amino-9-hydroxy-2-(3-methylphenyl)chromeno[4,3,2-de]-[1,6]naphthyridine-4-carbonitrile (4e, C<sub>22</sub>H<sub>14</sub>N<sub>4</sub>O<sub>2</sub>)** Yellow solid; m.p.: > 300 °C; IR (KBr):  $\bar{\nu}$  = 3487, 3328, 3294, 3168, 2206 cm<sup>-1</sup>; <sup>1</sup>H NMR (300 MHz, DMSO-*d*<sub>6</sub>):  $\delta$  = 10.67 (1H, s), 8.31–8.34 (1H, d, *J* = 8.7 Hz), 8.06–8.14 (3H, m), 7.36–7.42 (3H, m), 7.32 (1H, s), 6.85–6.88 (1H, d, *J* = 8.7 Hz), 6.30 (1H, s), 2.44 (3H, s) ppm; <sup>13</sup>C NMR (75 MHz, DMSO-*d*<sub>6</sub>):  $\delta$  = 162.44, 162.36, 162.16, 159.80, 155.87, 153.72,

139.37, 138.44, 138.25, 131.53, 128.95, 128.54, 127.04, 125.31, 117.10, 114.23, 109.36, 103.99, 103.83, 102.18, 76.10, 21, 65 ppm.

**5-Amino-9-hydroxy-2-(2-chlorophenyl)chromeno[4,3,2-de]-[1,6]naphthyridine-4-carbonitrile (4f, C<sub>21</sub>H<sub>11</sub>ClN<sub>4</sub>O<sub>2</sub>)** Yellow solid; m.p.: > 300 °C; IR (KBr):  $\bar{\nu}$  = 3461, 3358, 3233, 2210 cm<sup>-1</sup>; <sup>1</sup>H NMR (300 MHz, DMSO-*d*<sub>6</sub>):  $\delta$  = 10.77 (1H, s), 8.19–8.22 (1H, d, *J* = 9.0 Hz), 7.76 (1H, s), 7.64–7.68 (2H, m), 7.51–7.57 (3H, m), 7.12 (1H, s), 6.98 (1H, s), 6.92 (1H, s), 6.86–6.89 (1H, m) ppm; <sup>13</sup>C NMR (75 MHz, DMSO-*d*<sub>6</sub>):  $\delta$  = 163.67, 162.59, 162.21, 159.95, 155.87, 153.86, 139.71, 138.88, 131.85, 131.68, 131.09, 130.36, 127.82, 126.94, 117.00, 114.73, 114.51, 108.96, 108.27, 103.92, 102.15, 75.98 ppm.

**5-Amino-9-hydroxy-2-(2-bromophenyl)chromeno[4,3,2-de]-[1,6]naphthyridine-4-carbonitrile (4g, C<sub>21</sub>H<sub>11</sub>BrN<sub>4</sub>O<sub>2</sub>)** Yellow solid; m.p.: > 300 °C; IR (KBr):  $\bar{\nu}$  = 3461, 3351, 3228, 2217 cm<sup>-1</sup>; <sup>1</sup>H NMR (300 MHz, DMSO-*d*<sub>6</sub>):  $\delta$  = 10.96 (1H, s), 8.50 (1H, s), 8.30–8.34 (2H, m), 8.08 (1H, s), 7.68–7.71 (1H, d, *J* = 7.4 Hz), 7.41–7.51 (3H, m), 6.82–6.85 (1H, dd, *J* = 12.9, 2.1 Hz), 6.76–6.77 (1H, d, *J* = 2.1 Hz) ppm; <sup>13</sup>C NMR (75 MHz, DMSO-*d*<sub>6</sub>):  $\delta$  = 162.48, 162.16, 160.39, 159.76, 155.70, 153.71, 140.69, 139.78, 133.48, 131.13, 130.46, 127.18, 126.98, 122.76, 116.98, 114.23, 109.26, 104.04, 103.78, 102.44, 76.10 ppm.

**5-Amino-9-hydroxy-2-(4-bromophenyl)chromeno[4,3,2-de]-[1,6]naphthyridine-4-carbonitrile (4h, C<sub>21</sub>H<sub>11</sub>BrN<sub>4</sub>O<sub>2</sub>)** Yellow solid; m.p.: > 300 °C; IR (KBr):  $\bar{\nu}$  = 3475, 3365, 3156, 2209 cm<sup>-1</sup>; <sup>1</sup>H NMR (300 MHz, DMSO-*d*<sub>6</sub>):  $\delta$  = 10.72 (1H, s), 8.35 (1H, s), 8.30–8.33 (2H, d, *J* = 8.4 Hz), 8.13 (1H, s), 7.75–7.78 (2H, m), 7.44 (2H, s), 6.86–6.89 (1H, dd, *J* = 12.9, 2.4 Hz), 6.80–6.81 (1H, d, *J* = 2.4 Hz) ppm; <sup>13</sup>C NMR (75 MHz, DMSO-*d*<sub>6</sub>):  $\delta$  = 162.50, 162.19, 161.03, 159.82, 155.84, 153.78, 139.77, 137.60, 132.12, 130.02, 127.16, 124.86, 116.99, 114.32, 109.30, 103.85, 102.86, 76.01 ppm.

**5-Amino-9-hydroxy-2-(4-chlorophenyl)chromeno[4,3,2-de]-[1,6]naphthyridine-4-carbonitrile (4i, C<sub>21</sub>H<sub>11</sub>ClN<sub>4</sub>O<sub>2</sub>)** Yellow solid; m.p.: > 300 °C; IR (KBr):  $\bar{\nu}$  = 3461, 3353, 3216, 2210 cm<sup>-1</sup>; <sup>1</sup>H NMR (300 MHz, DMSO-*d*<sub>6</sub>):  $\delta$  = 10.69 (1H, s), 8.21–8.36 (2H, m), 8.07 (1H, s), 7.40–7.60 (4H, m), 6.77–6.86 (3H, m) ppm; <sup>13</sup>C NMR (75 MHz, DMSO-*d*<sub>6</sub>):  $\delta$  = 162.45, 162.15, 161.31, 160.84, 159.74, 155.76, 153.71, 137.18, 135.87, 129.73, 129.11, 128.97, 127.05, 116.79, 114.27, 109.25, 103.80, 102.26, 76.05 ppm.

**5-Amino-9-hydroxy-2-(3-bromophenyl)chromeno[4,3,2-de]-[1,6]naphthyridine-4-carbonitrile (4j, C<sub>21</sub>H<sub>11</sub>BrN<sub>4</sub>O<sub>2</sub>)** Yellow solid; m.p.: > 300 °C; IR (KBr):  $\bar{\nu}$  = 3463, 3350, 3229, 2217 cm<sup>-1</sup>; <sup>1</sup>H NMR (300 MHz, DMSO-*d*<sub>6</sub>):  $\delta$  = 10.67 (1H,

s), 8.50 (1H, s), 8.29–8.32 (2H, d, *J* = 7.2 Hz), 8.07 (2H, s), 7.68–7.71 (1H, d, *J* = 7.8 Hz), 7.45–7.51 (1H, t, *J* = 7.8 Hz), 7.41 (2H, s), 6.82–6.84 (1H, d, *J* = 8.1 Hz), 6.76 (1H, s) ppm; <sup>13</sup>C NMR (75 MHz, DMSO-*d*<sub>6</sub>):  $\delta$  = 162.47, 162.15, 160.37, 159.75, 155.69, 153.70, 140.68, 139.76, 133.47, 131.12, 130.46, 127.17, 126.98, 122.75, 116.98, 114.22, 109.26, 104.08, 103.77, 102.43, 76.05 ppm.

**5-Amino-9-hydroxy-2-(2-methoxyphenyl)chromeno[4,3,2-de]-[1,6]naphthyridine-4-carbonitrile (4k, C<sub>22</sub>H<sub>14</sub>N<sub>4</sub>O<sub>3</sub>)** Yellow solid; m.p.: > 300 °C; IR (KBr):  $\bar{\nu}$  = 3484, 329, 3160, 2220 cm<sup>-1</sup>; <sup>1</sup>H NMR (300 MHz, DMSO-*d*<sub>6</sub>):  $\delta$  = 10.68 (1H, s), 7.79–8.08 (3H, q), 7.42–7.51 (3H, m), 7.09–7.22 (2H, m), 6.82–6.88 (2H, m), 3.89 (3H, s) ppm; <sup>13</sup>C NMR (75 MHz, DMSO-*d*<sub>6</sub>):  $\delta$  = 162.78, 162.31, 162.07, 159.87, 157.73, 155.94, 153.78, 137.94, 131.60, 131.44, 128.89, 126.51, 121.07, 117.16, 114.44, 112.55, 109.16, 108.58, 103.96, 101.85, 75.98, 56.29 ppm.

**5-Amino-9-hydroxy-2-(2,3-dimethoxyphenyl)chromeno[4,3,2-de]-[1,6]naphthyridine-4-carbonitrile (4l, C<sub>23</sub>H<sub>16</sub>N<sub>4</sub>O<sub>4</sub>)** Yellow solid; m.p.: > 300 °C; IR (KBr):  $\bar{\nu}$  = 3480, 3338, 3225, 2211 cm<sup>-1</sup>; <sup>1</sup>H NMR (300 MHz, DMSO-*d*<sub>6</sub>):  $\delta$  = 10.72 (1H, s), 8.11–8.14 (1H, d, *J* = 8.7 Hz), 7.79 (1H, s), 7.74 (2H, s), 7.22–7.30 (3H, m), 6.85–6.91 (2H, m), 3.90 (3H, s), 3.82 (3H, s) ppm; <sup>13</sup>C NMR (75 MHz, DMSO-*d*<sub>6</sub>):  $\delta$  = 163.37, 162.42, 162.13, 159.93, 155.88, 153.82, 153.44, 147.37, 138.57, 134.93, 126.67, 124.51, 122.62, 117.13, 114.53, 114.49, 109.12, 107.94, 103.97, 102.00, 75.97, 21.65 ppm.

**5-Amino-9-hydroxy-2-(3,4,5-trimethoxyphenyl)chromeno[4,3,2-de]-[1,6]naphthyridine-4-carbonitrile (4m, C<sub>24</sub>H<sub>18</sub>N<sub>4</sub>O<sub>5</sub>)** Yellow solid; m.p.: > 300 °C; IR (KBr):  $\bar{\nu}$  = 3382, 3295, 3191, 2297, 2206 cm<sup>-1</sup>; <sup>1</sup>H NMR (300 MHz, DMSO-*d*<sub>6</sub>):  $\delta$  = 10.67 (1H, s), 8.29–8.32 (1H, d, *J* = 8.4 Hz), 7.96 (1H, s), 7.60 (2H, s), 7.36 (2H, s), 6.76–6.87 (3H, m), 3.91 (6H, s), 3.78 (3H, s) ppm; <sup>13</sup>C NMR (75 MHz, DMSO-*d*<sub>6</sub>):  $\delta$  = 162.28, 162.05, 161.55, 159.66, 155.58, 153.65, 153.33, 140.20, 139.20, 133.68, 127.06, 116.95, 114.08, 109.34, 105.48, 103.79, 103.58, 101.96, 76.08, 60.59, 56.40 ppm.

**5-Amino-9-hydroxy-2-(3,4-dimethoxyphenyl)chromeno[4,3,2-de]-[1,6]naphthyridine-4-carbonitrile (4n, C<sub>23</sub>H<sub>16</sub>N<sub>4</sub>O<sub>4</sub>)** Yellow solid; m.p.: > 300 °C; IR (KBr):  $\bar{\nu}$  = 3459, 3387, 3212, 2295, 2210 cm<sup>-1</sup>; <sup>1</sup>H NMR (300 MHz, DMSO-*d*<sub>6</sub>):  $\delta$  = 10.67 (1H, s), 8.36–8.39 (1H, d, *J* = 8.7 Hz), 7.96–8.06 (3H, m), 7.38 (2H, s), 7.09–7.12 (2H, d, *J* = 8.1 Hz), 6.72–6.97 (2H, m), 3.91 (3H, s), 3.87 (3H, s) ppm; <sup>13</sup>C NMR (75 MHz, DMSO-*d*<sub>6</sub>):  $\delta$  = 162.30, 162.11, 161.96, 159.75, 155.85, 153.74, 151.64, 149.18, 139.17, 130.94, 127.14, 121.53, 117.09, 114.72,

114.18, 111.90, 111.28, 109.45, 103.87, 103.30, 101.81, 76.05, 56.06 ppm.

**5-Amino-9-hydroxy-2-(2,5-dimethoxyphenyl)-chromeno[4,3,2-de][1,6]naphthyridine-4-carbonitrile (4o, C<sub>23</sub>H<sub>16</sub>N<sub>4</sub>O<sub>4</sub>)** Yellow solid; m.p.: > 300 °C; IR (KBr):  $\bar{\nu}$  = 3472, 3318, 3217, 2926, 2226 cm<sup>-1</sup>; <sup>1</sup>H NMR (300 MHz, DMSO-*d*<sub>6</sub>):  $\delta$  = 10.72 (1H, s), 8.08–8.11 (1H, d, *J* = 8.1 Hz), 7.95 (1H, s), 7.42–7.44 (3H, m), 6.85–6.91 (4H, m), 3.85 (3H, s), 3.99 (3H, s) ppm; <sup>13</sup>C NMR (75 MHz, DMSO-*d*<sub>6</sub>):  $\delta$  = 162.39, 162.37, 162.08, 159.87, 155.86, 153.82, 153.66, 152.07, 138.15, 129.60, 126.54, 117.06, 116.78, 116.39, 114.51, 114.21, 109.17, 108.45, 104.00, 101.95, 76.10, 56.99, 55.99 ppm.

**5-Amino-9-hydroxy-2-(3,4-dihydroxyphenyl)-chromeno[4,3,2-de][1,6]naphthyridine-4-carbonitrile (4p, C<sub>21</sub>H<sub>12</sub>N<sub>4</sub>O<sub>4</sub>)** Yellow solid; m.p.: > 300 °C; IR (KBr):  $\bar{\nu}$  = 3494, 3430, 3385, 3252, 2194 cm<sup>-1</sup>; <sup>1</sup>H NMR (300 MHz, DMSO-*d*<sub>6</sub>):  $\delta$  = 10.67 (1H, s), 9.57 (1H, s), 9.28 (1H, s), 8.36–8.38 (1H, d, *J* = 5.7 Hz), 8.03 (1H, s), 7.90–7.91 (1H, d, *J* = 1.8 Hz), 7.75–7.78 (1H, dd, *J* = 12.3, 4.5 Hz), 7.37 (2H, s), 6.83–6.93 (3H, m) ppm; <sup>13</sup>C NMR (75 MHz, DMSO-*d*<sub>6</sub>):  $\delta$  = 162.70, 162.24, 162.17, 159.78, 156.01, 153.73, 148.94, 145.94, 138.91, 129.93, 127.03, 120.45, 117.28, 115.98, 115.60, 114.26, 109.48, 103.88, 103.19, 101.63, 76.00 ppm.

**Acknowledgements** We gratefully appreciate the University of Sistan and Baluchestan Research Councils for the financial support of this work.

## References

- Lang H (2018) Polyhedron 139:50
- Dehbanipour Z, Moghadam M, Tangestaninejad S, Mirkhani V, Mohammadpoor-Baltork I (2017) J Organomet Chem 853:5
- Abubekerev M, Khan SI, Diaconescu PL (2017) Organometallics 36:4394
- Fernandes AC, Florindo P, Pereira DM, Borrallho PM, Rodrigues CMP, Piedade MMF (2014) J Med Chem 58:4339
- Seok An G, Choi SW, Chae DH, Lee HS, Kim H-J, Kim Y, Jung Y-G, Choi S-C (2017) Ceram Int 43:12888
- Hervault A, Thanh NTK (2017) Nanoscale 6:11553
- Lamei K, Eshghi H, Bakavoli M, Rostamnia S (2017) Appl Organomet Chem 31:e3743
- Wu W, Jiang CZ, Roy VAL (2017) Nanoscale 8:19421
- Mrówczyński R (2017) ACS Appl Mater Interfaces 10:7541
- Hajipour AR, Check M, Khorsandi Z (2017) Appl Organomet Chem 31:e3769
- Kharissova OV, Dias HVR, Kharisov BI (2017) RSC Adv 5:6695
- Naeimi H, Aghaseyed Karimi D (2017) New J Chem 39:9415
- Taheri N, Heidarizadeh F, Kiasat A (2017) J Magn Magn Mater 428:481
- Sadjadi S, Malmir M, Heravi MM (2017) RSC Adv 7:36807
- Saravanan P, Jayamoorthy K, Anandakumar S (2016) J Lumin 178:241
- Wang D, Deraedt C, Ruiz J, Astruc D (2015) Acc Chem Res 48:1871
- Ho KM, Li P (2008) Langmuir 24:1801
- Azizi K, Heydari A (2014) RSC Adv 4:8812
- Tsuji K, Injuk J, Grieken RV (2014) X-ray spectrometry: recent technological advances. John Wiley & Sons, Chichester
- Singh P, Ebenso EE, Olasunkanmi LO, Obot IB, Quraishi MA (2014) J Phys Chem C 120:3408
- Wu H, Lin W, Wan Y, Xin H-Q, Shi D-Q, Shi Y-H, Yuan R, Bo R-C, Yin W (2010) J Comb Chem 12:31
- Dandia A, Parewa V, Gupta SL, Sharma A, Rathore KS, Sharma A, Jain A (2015) Catal Commun 61:88